



## The palaeomagnetism of glauconitic sediments

Pontus C. Lurcock<sup>a,\*</sup>, Gary S. Wilson<sup>b</sup>

<sup>a</sup> Department of Geology, University of Otago, PO Box 56, Dunedin, New Zealand

<sup>b</sup> Marine Science Department, University of Otago, PO Box 56, Dunedin, New Zealand

### ARTICLE INFO

#### Article history:

Received 3 September 2012

Received in revised form 11 June 2013

Accepted 22 June 2013

Available online 6 July 2013

#### Keywords:

glaucony  
palaeomagnetism  
rock magnetism  
magnetic mineralogy  
diagenesis  
marine sediments

### ABSTRACT

The palaeoenvironmental significance of glaucony has long been appreciated, but accurate palaeomagnetic dating of events recorded by glauconitic horizons requires an understanding of how glauconitic sediments acquire a remanent magnetization. Pure glauconitic minerals are paramagnetic, but glauconite grains are large and slow-forming (over periods that can exceed 100 kyr), with complex and variable morphologies. It is, thus, possible that small magnetic grains within glaucony particles may carry a significant fraction of the remanence in weakly magnetized sediments. Any remanence carried by glauconitic grains may therefore represent the geomagnetic field at a time significantly later than the time of deposition, or a time-averaged signal over some or all of the formation period. We investigated this problem using weakly magnetic Palaeocene glauconitic siltstones from southern New Zealand. We disaggregated the rock and separated it magnetically into glauconitic and non-glauconitic fractions. Results from stepwise isothermal remanent magnetization (IRM) acquisition, alternating-field demagnetization, temperature dependence of magnetic susceptibility, and stepwise thermal demagnetization of a triaxial IRM were used to demonstrate that the remanent magnetization is carried by single-domain or pseudo-single-domain magnetite in the non-glauconitic sediment fraction, and that the glauconite grains themselves make no contribution to the remanent magnetization. However, accurate measurement of the primary remanence is complicated by a strong viscous overprint and mineral alteration during thermal demagnetization studies. Identification of magnetite as the remanence carrier in sediments within a reducing diagenetic environment gives confidence that the remanence has a depositional origin. Glauconite does not carry a remanence; therefore, its effect is to dilute and weaken the overall magnetization. Furthermore, the use of rock magnetic parameters may be problematic when glauconite concentrations are (as in the studied sediments) orders of magnitude greater than remanence carrier concentrations, because in such cases the glauconite susceptibility can dominate that of the remanence carriers.

© 2013 Elsevier B.V. All rights reserved.

### 1. Introduction

Glaucony is found worldwide in late pre-Cambrian to modern marine sediments (Odin and Matter, 1981); it forms diagenetically at the sediment–water interface and can provide valuable palaeoenvironmental data. Glauconitic horizons have long been interpreted as indicators of reduced or interrupted deposition (Goldman, 1922), and in sequence stratigraphy they have generally been associated with sea level transgressions (e.g. Mitchum and Van Wagoner, 1991). Glauconite formation is sensitive to a range of environmental conditions, including sediment supply (Goldman, 1922), water depth (Hesselbo and Huggert, 2001), and water temperature (Huggert, 2005); glauconitic horizons can, thus, record events such as eustatic sea level fluctuations and variations in ocean circulation, and provide valuable information in palaeoenvironmental and palaeoclimatic studies.

For glauconitic strata, as for other sediments, magnetostratigraphy has the potential to provide accurate age constraints, but palaeomagnetic analysis of glauconitic sediments is not straightforward. Odin and Matter (1981) proposed a model of glauconite formation in which grains form and mature at the sea floor over time periods often exceeding 100 kyr and sometimes estimated up to 5 Myr (Huggert, 2005). This model has been applied to improve sequence stratigraphic interpretations of glauconitic horizons (Amorosi, 1995), but their mode of formation also has important consequences for magnetostratigraphic interpretation. Glauconite has traditionally been classed as purely paramagnetic, but the sensitivity of modern magnetometers permits measurement of weakly magnetized (<50  $\mu\text{A}/\text{m}$ ) sediments that would previously not have been considered suitable for palaeomagnetic research.

In Odin and Matter's (1981) model, glauconitization occurs in semi-enclosed sea-floor environments on a variety of substrates, most often porous grains of 50–1000  $\mu\text{m}$  in diameter. Substrates include shell fragments, foraminiferal tests, mica flakes, and faecal pellets. Glauconitization begins with the growth of glauconitic smectite in pore spaces. As the pores are filled, the initial substrate often begins to dissolve. Continued

\* Corresponding author.

E-mail addresses: [pont@talvi.net](mailto:pont@talvi.net) (P.C. Lurcock), [gary.wilson@otago.ac.nz](mailto:gary.wilson@otago.ac.nz) (G.S. Wilson).

glaucanization destroys the grain's primary texture and produces a characteristic bulbous, cracked habit. The final stage adds a smooth outer crust of glauconitic minerals, giving the completely evolved grain a more rounded shape. If magnetic remanence is carried by particles incorporated into glauconite during its development, the magnetization of the sediment may not reflect the Earth's magnetic field at the time of deposition: it may instead hold a magnetic signal from a later time, or a mixed signal averaged over an extended time period. The present study was motivated by the need to provide accurate age control on Palaeogene glauconitic horizons from New Zealand.

We address two questions: first, can highly glauconitic sediments yield a reliable magnetic remanence? Second, how should such a remanence be interpreted palaeomagnetically?

**2. Material and methods**

We compared the rock magnetic behaviour of four groups of samples.

- (1) Samples from within a well-defined highly glauconitic horizon.
- (2) Samples from the less glauconitic zones immediately above and below this horizon.
- (3) Artificial concentrates of glauconitic grains from the glauconitic horizon.
- (4) Artificial concentrates of non-glauconitic grains from the glauconitic horizon.

These sample groupings allow us to answer two questions. First, how does the magnetic behaviour of glauconitic and non-glauconitic sediments differ? Second, what is the magnetic role of the glauconitic grains themselves?

We selected a glauconitic horizon exposed at Fairfield Quarry near Dunedin (southeastern South Island, New Zealand; 45°53'34" S, 170°24'36" E). The horizon occurs within the lower Abbotsford Formation (McMillan and Wilson, 1997) and is of Palaeocene age. We drilled standard palaeomagnetic core samples from this horizon, and from the less glauconitic zones immediately above and below it. The glauconitic horizon was ~1 m thick, and the underlying and overlying intervals were, respectively, ~2 m and ~3.5 m thick. We also

collected bulk sediment samples from the same stratigraphic levels; these samples were used to create the glauconitic and non-glauconitic separates.

We analysed three types of sample: palaeomagnetic drill cores; powder samples, prepared directly from crushed bulk samples or from magnetic mineral separates; and artificial cube samples made from cemented powders. Producing artificially cemented cubes allowed us to apply bulk magnetic techniques requiring discrete, orientable specimens. Identical treatment protocols could thus be applied to the unprocessed drill cores and to the cubes, allowing direct comparisons of magnetic behaviour between bulk material and separates. Our sampling scheme is summarized in Fig. 1. Note that for the D-series and C-series samples, each sample code denotes four sister samples; unless otherwise stated, all numerical results presented in this paper for 'C' and 'D' samples represent the mean of four samples with the same sample code.

D-series samples were collected directly from the outcrop using a drill with a water-cooled 25-mm diamond-tipped stainless-steel bit, and were cut into standard 22-mm palaeomagnetic specimens using a diamond-edged copper saw. We produced P-series samples by manually disaggregating bulk samples. We then produced separates from site 2 (glauconitic zone) sediment by sieving and magnetic separation: we wet-sieved the disaggregated material using a 62 µm mesh and dried the coarse fraction at room temperature. We then dry-sieved this material to separate it into 62–180 µm and 180–500 µm fractions (all the grains are smaller than 500 µm). Size fractionation allowed us to investigate grain size effects on magnetic properties; it is also known to increase the efficiency of magnetic separation (Odin, 1982, p. 392). We magnetically separated the sized glauconitic material using a Frantz-type isodynamic separator with a current of 0.55 A, a longitudinal dip of 15°, and a transverse tilt of 8°. Magnetic separation is commonly used for glauconite extraction (e.g. Amorosi et al., 2007) and owes its effectiveness to the high paramagnetic susceptibility of glauconite. Bentor and Kastner (1965) reported a glauconite susceptibility of around  $4.3 \times 10^{-4}$  (SI); while this is much lower than susceptibilities of ferrimagnetic minerals (e.g. magnetite, 1–5.7 SI), it is much higher than many common diamagnetic and paramagnetic minerals (e.g. quartz,  $-1.3\text{--}1.7 \times 10^{-5}$  SI) (Hunt et al., 1995). Our glauconitic separates contained above 90% glauconite, and the non-glauconitic

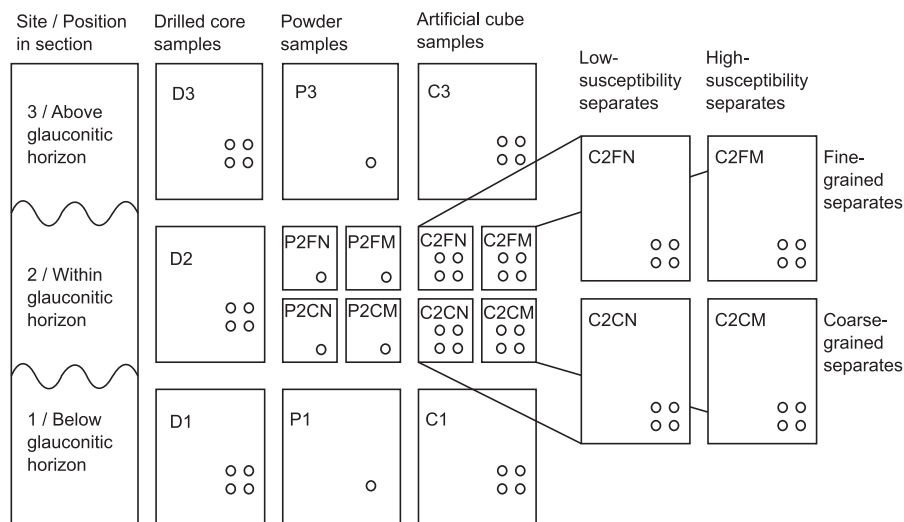


**Fig. 1.** Summary of the sample groups used in this study. Each box corresponds to a uniform sample group, and is labelled with its sample code; the C2 samples are depicted twice, to allow annotation of the different grain size and magnetic susceptibility fractions. The high-susceptibility separates were expected to contain higher concentrations of glauconite than the low-susceptibility separates. Sample groups are identified by a code of 2–4 characters, constructed as follows: (1) Sample type: D[ri]ll core, C[ube], P[owder]; (2) position relative to glauconitic horizon: 1 below, 2 within, 3 above; (3) size fraction: F[ine], C[oarse]; (4) susceptibility fraction: M high (glauconitic), N low (non-glauconitic). Fractionation was only performed for samples from position 2 (within the glauconitic horizon). Each small circle corresponds to a single physical sample, so each 'C' or 'D' sample code denotes a set of four sister samples.

**Table 1**  
Rock magnetic parameters for the discrete sample groups.

Sample group	$B_{cr}$ (mT)	$B'_{cr}$ (mT)	MDF (mT)	SIRM (mA/m)	NRM ( $\mu$ A/m)
D1	42.8	48.5	28.3	163	130
C1	43.0	49.5	28.5	199	–
D3	42.3	48.2	27.9	162	69
C3	41.5	47.7	27.6	170	–
C2CN	44.5	51.8	28.8	127	–
C2FN	44.6	52.0	29.4	110	–
D2	41.1	47.1	25.4	86	121
C2CM	46.7	56.0	28.9	52	–
C2FM	42.1	49.7	26.8	66	–

Parameters were determined as mean values from four sister samples. Parameter definitions:  $B_{cr}$  remanent coercivity;  $B'_{cr}$  remanent coercivity of acquisition; MDF median destructive field of IRM; SIRM saturation isothermal remanent magnetization; NRM natural remanent magnetization. (C-series samples were artificially produced in a shielded room with an ambient field strength below 150 nT, so only the D-series samples had NRM.)

separates contained less than 50% glauconite; this difference was considered sufficient to determine the magnetic role of the glauconitic grains.

C-series samples were produced by cementing disaggregated material into solid cubes. We mixed the powder with aqueous sodium silicate solution to produce a paste, which we formed into 8 cm<sup>3</sup> cubes using IODP sample cubes as moulds. Sodium silicate has been shown to have no effect on magnetic remanence properties, even after heat treatment (Kostadinova et al., 2004).

We made several rock magnetic and mineralogical analyses on the sampled material to identify the minerals that carry the magnetization. In the treatments listed below, all magnetic moment measurements were made on a 2-G Enterprises cryogenic magnetometer with three Applied Physics Model 581 SQUID pick-up coils.

- (1) *Measurement of the natural remanent magnetization (NRM)* followed by stepwise demagnetization using a 2G600 triaxial sample degaussing system. We increased the alternating field in 5 mT steps from 0 to 50 mT, then in 10 mT steps to 100 mT. A final alternating field of 120 mT was applied to demagnetize the samples as fully as possible before IRM acquisition.
- (2) *Stepwise acquisition of an isothermal remanent magnetization (IRM)*, imparted using an ASC Scientific IM-10 impulse magnetizer. We increased the magnetic field in 5 mT steps from 0 to 90 mT, then in 10 mT steps to 160 mT; subsequent steps were 180, 200, 250, 300, 350, 400, 450, 500, 600, 800, and 1000 mT.
- (3) *Stepwise backfield demagnetization of the IRM* ('DC demagnetization'). Field strength was increased from 0 mT in the same steps as for IRM acquisition, but the treatment was stopped once the initial IRM had been entirely removed.

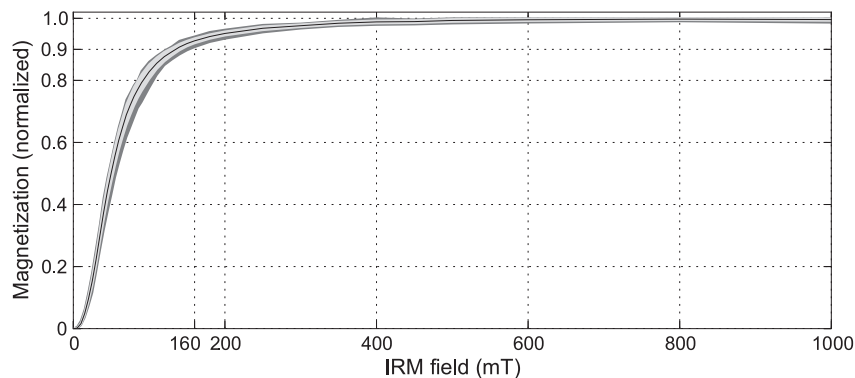


**Fig. 2.** Normalized IRM acquisition curves for all samples studied. All remanent coercivity spectra are similar. The spread of data is shown across all individual samples, not across averaged sample groups. The dark grey area represents the full range of values; the light grey area represents one standard deviation either side of the mean; the black line is the mean. The samples acquired over 90% of their saturation remanence by 160 mT.

- (4) *Stepwise AF demagnetization of a 1 T IRM* in 5 mT steps from 0 to 50 mT followed by 10 mT steps from 50 to 150 mT.
- (5) *Temperature dependence of magnetic susceptibility (TDMS)*. We measured TDMS on the powder samples using an Agico MFK-1A Kappabridge operating at 976 Hz, with a CS-3 furnace. Heating was carried out in an argon atmosphere. Each sample was repeatedly heated and cooled in seven successive cycles. The peak temperature was increased for each cycle, from 100 °C to 700 °C in 100 °C steps. This procedure was described by Hrouda (2003), and is useful for identifying in which temperature intervals heating-induced mineral alteration has occurred.
- (6) *Stepwise thermal demagnetization of a triaxial IRM* using the technique described by Lowrie (1990). We first applied 1 T, 0.4 T, and 0.12 T IRMs to each sample in mutually orthogonal directions. These IRMs are independent of each other, so they divide the magnetization into three remanent coercivity bands. We then thermally demagnetized the samples in 25 °C steps from 25 °C to 775 °C, with a heating time of 40 min at each step, to determine a thermal unblocking spectrum for each coercivity band. Heating was performed in an ASC Scientific TD-48SC thermal specimen demagnetizer.
- (7) *Optical microscopy* on thin sections, using an Olympus BX-41 polarizing microscope with a reflected-light illuminator and a Zeiss AxioCam MRc camera.
- (8) *Electron microscopy and electron probe microanalysis (EPMA)* on carbon-coated thin sections, using a JEOL JXA-8600 electron microprobe analyser.

We also performed stepwise thermal demagnetization of NRM on core samples drilled from the same stratigraphic heights as the samples used in the main study. We demagnetized these samples at 25 °C intervals from 25 °C, stopping treatment when thermal alteration obscured the remaining magnetization.

### 3. Results

#### 3.1. Isothermal remanent magnetization

Magnetic parameters determined from the IRM experiments and other measurements are listed in Table 1. Although there is considerable variation between the saturation IRM (SIRM) values of the samples, the normalized IRM acquisition curves are similar in shape (Fig. 2), which indicates that the remanence carriers are the same for all sample groups and that only their concentration varies.

The gradient of the IRM acquisition curves is plotted against the logarithm of the applied field in Fig. 3. Plotting the gradient rather than the IRM allows coercivity components to be more easily distinguished, because the field intervals where most of the IRM is acquired

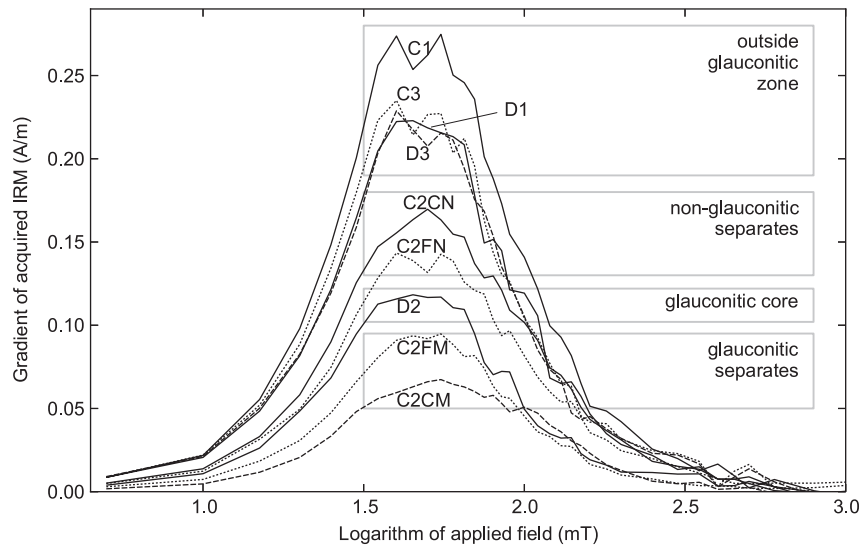


**Fig. 3.** Plot of gradient of magnetization from IRM acquisition curves against the logarithm of applied field for each sample group. Each line represents the mean magnetization of four sister samples.

appear as peaks. In this plot, the area under the curves is proportional to the SIRM of each sample group.

It can be seen from Fig. 3, and from the values in Table 1, that SIRM is inversely correlated with glauconite content: the highest SIRMs are produced in samples from positions 1 and 3, outside the glauconitic zone, while the highly glauconitic material from position 2 has a much lower SIRM. The same relationship is evident in the magnetic separates: the glauconitic separates have a lower SIRM than the non-separated source material of the D2 samples, while the non-glauconitic separates have a higher SIRM than the D2 samples.

### 3.1.1. Quantitative unmixing of IRM curves

Following the work of Robertson and France (1994), IRM acquisition curves have often been used to separate components from mixtures of remanence carriers, and quantitative techniques have been developed (e.g. Kruiver et al., 2001) to separate measured IRM curves into components corresponding to the individual magnetic minerals. We used the IRMunmix program of (Heslop et al., 2002) to unmix the IRM curves into sums of cumulative log-Gaussian (CLG) functions, each representing an individual magnetic phase. Two examples of CLG curve fitting are shown in Fig. 4.

In all cases, the IRM acquisition curves can be represented as the sum of two extensively overlapping CLG curves. A single CLG curve always provides a reasonable fit, but in most cases it provides a slightly worse fit than the two-component fit; the exception was sample

group C2CM, where the one- and two-component fits were practically indistinguishable. Heslop et al. (2002) discussed caveats about the accuracy of CLG fitting when (as is the case here) there is extensive overlap between the components. Egli (2003) questioned whether a CLG curve is always sufficient to describe a single magnetic mineral. It is, thus, unclear whether the IRM data represent a single magnetic mineral, or two minerals with similar remanent coercivities. The fact that the single-component fit is always close to – and, for group C2CM, practically identical to – the two-component fit suggests that the two components may be an artefact of the model and fitting procedure.

### 3.1.2. Mineral identification

Rock magnetic parameters for each sample group are listed in Table 1, including: the remanent coercivity  $B_{cr}$  (the reverse field which reduces the remanent magnetization of a saturated sample to zero); the remanent coercivity of acquisition  $B'_{cr}$  (the field which magnetizes a sample to one half of its saturation magnetization); and the MDF of IRM (the alternating field which demagnetizes a saturated sample to one-half of its SIRM). The values for these parameters are all consistent with published values for magnetite (Peters and Dekkers, 2003). The IRM data also rule out haematite and goethite, both of which have far higher remanent coercivities than any of the analysed samples. Pyrrhotite and greigite generally have higher remanent coercivities than magnetite (Peters and Dekkers, 2003), but

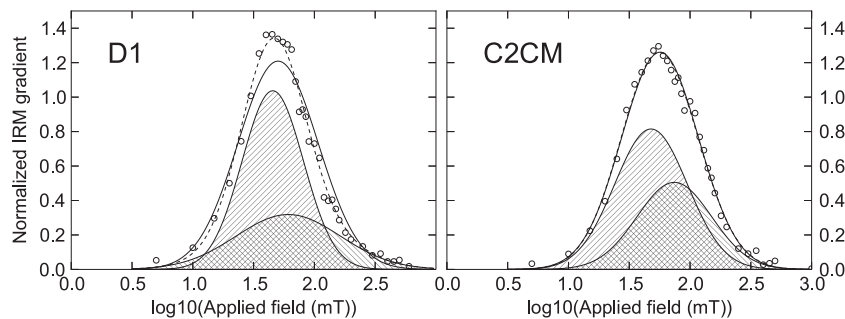


**Fig. 4.** Two examples of fitting cumulative log-Gaussian (CLG) curves to IRM acquisition data. The circular data points define the slope of the measured IRM acquisition curve. The dashed line represents the best two-component fit; it is calculated as the sum of two CLG functions, which are shown as overlapping hatched areas. The best-fitting single-component fit is shown as a solid line. In the right-hand figure (sample group C2CM) the single-component and two-component fits represent the data equally well, so that the solid line obscures the dashed line.

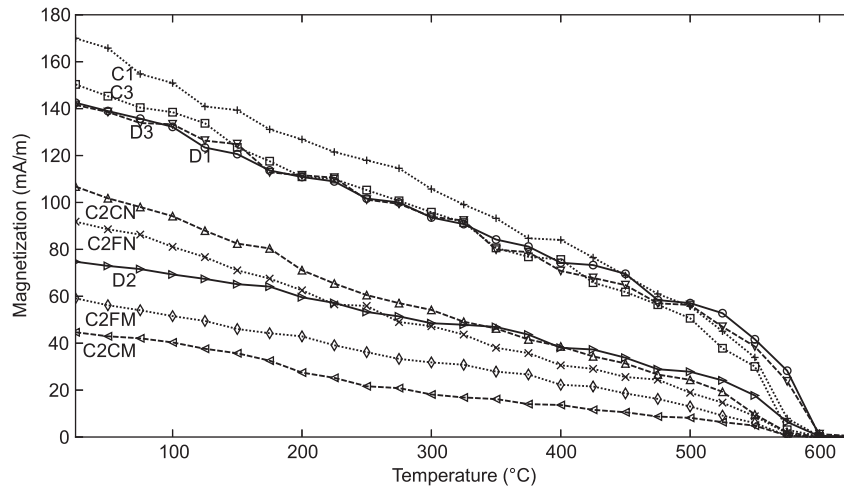


Fig. 5. Thermal demagnetization of the 0.12 T component of a triaxial IRM for all discrete sample sets.

their ranges overlap with those of magnetite and these minerals cannot be ruled out on the basis of IRM data alone; if the two-component CLG fits are used, it is possible to interpret the curves as reflecting a mixture of magnetite with one of these higher-coercivity minerals.

### 3.2. Stepwise thermal demagnetization of a triaxial IRM

As would be expected from the IRM acquisition curves, the majority of the imparted IRM was aligned with the 0.12 T field in all measured samples. Typically the 0.12 T component accounted for around 75% of the total remanence, with the 0.4 T component giving 15–20% and the 1 T component responsible for 5–10% of the remanence.

Non-normalized demagnetization curves for the 0.12 T component of each sample group are shown in Fig. 5; curves for the 0.4 T and 1 T components are similar to those of the 0.12 T components. All coercivity components of all samples have similar behaviour: a steady decrease in magnetization, with complete demagnetization achieved within the 550–600 °C interval. This interval is consistent with a remanence carried by magnetite, which has a Curie temperature of 580 °C. Some samples were almost completely demagnetized at 575 °C, which suggests a slightly lower Curie temperature. This can be explained by a small amount of cation substitution by, for example, titanium.

The three-axis IRM demagnetization curves thus support the IRM data in providing evidence that magnetite dominates the magnetization of the studied sediments. The curves also exclude other minerals consistent with the IRM data – greigite and pyrrhotite – because both of these minerals lose their magnetization well below 580 °C (e.g. Dekkers, 1989; Roberts et al., 2011b).

### 3.3. Temperature dependence of magnetic susceptibility

TDMS data allow disordering temperatures (i.e. Curie or Néel points) of magnetic minerals to be observed as sharp drops in susceptibility during heating. Interpretation of TDMS results is complicated by heating-induced mineral alteration, mainly in the 400–700 °C temperature range (Fig. 6). While alteration doubtless also occurred during thermal demagnetization of IRMs, it did not cause any problems because demagnetization was performed in a zero field oven and any alteration products would thus carry a negligible remanence. During heating to 700 °C, each sample has a strong Hopkinson (1889) peak in the 400–600 °C range, with susceptibility falling to zero beyond the peak. This indicates a mineral with a disordering temperature above 500 °C. Exact determination of these temperatures is impractical: the Hopkinson peaks are broad, which suggests either a mixture of magnetic minerals or a mixture of grain sizes. The almost complete loss of susceptibility just below 600 °C, and the large increases in room-temperature susceptibility after the later heating steps, are consistent with the formation of magnetite during heating. Pyrite, which was observed in the samples (see Section 3.5), is a likely source material for magnetite formed during heating in argon (Li and Zhang, 2005; Wang et al., 2008). Thermal alteration limits the usefulness of determining accurate disordering temperatures because it is unclear whether the Hopkinson peaks correspond to a mineral originally present in the sample.

TDMS data are still valuable, however, because they allow exclusion of some minerals from consideration. Most obviously, the lack of susceptibility above 600 °C excludes haematite, which is consistent with IRM acquisition and thermal demagnetization results; it also excludes maghaemite. The 400 °C heating step is also useful for excluding

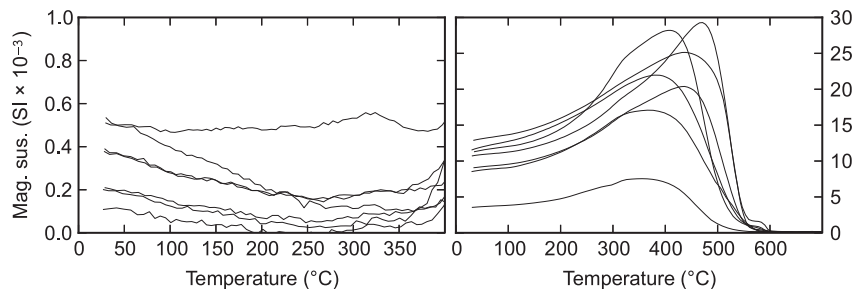


Fig. 6. Temperature dependence of magnetic susceptibility for all samples in the 400 °C (left) and 700 °C (right) heating steps. Strong Hopkinson peaks are visible in the 400–600 °C temperature range and no susceptibility signal is evident above 600 °C. No significant Hopkinson peaks are visible during the 400 °C heating step. The 400 °C curves differ from the corresponding parts of the 700 °C curves due to thermal alteration above 400 °C. Note the different vertical scales.

pyrrhotite, greigite, and goethite, all of which would cause a sharp susceptibility drop below this temperature.

### 3.4. Alternating-field demagnetization of IRM

The effect of stepwise AF demagnetization on a 1 T IRM is shown in Fig. 7 for each sample group. As is the case for the IRM acquisition data, the curves have similar shapes but have highly variable SIRM values. The curves all have an asymmetrically sigmoidal shape: the gradient steepens after the first demagnetization step, then the curve inflects and the gradient shallows gradually at subsequent steps. Reference plots of AF demagnetization for different minerals (e.g. Symons and Cioppa, 2000; Dunlop and Özdemir, 1997, p. 291) indicate that single-domain (SD) magnetite produces sigmoidal curves, whereas multi-domain (MD) magnetite gives rise to more hyperbolically shaped curves with no inflection. These AF results thus indicate the presence of SD or pseudo-single-domain (PSD) magnetite in the samples.

We calculated median destructive field (MDF) values from the AF demagnetization curves; the values are given in Table 1 and are consistent with previously measured MDF values for SD and PSD magnetites (Dunlop, 1986).

### 3.5. Microscopy and electron probe microanalysis

Thin sections were prepared from all sample groups. We examined these under optical and electron microscopes and found the extensive presence of pyrite with a variety of morphologies. EPMA analysis of 42 opaque grains confirmed that they are all stoichiometric pyrite. No remanence-carrying minerals were observed; this is consistent with the low magnetite concentration indicated by the SIRMs, which gives a correspondingly low likelihood of direct observation of magnetite grains in thin section.

### 3.6. Stepwise demagnetization of NRM

The rock magnetic data indicated that the samples were capable of retaining a primary palaeomagnetic signal. However, the weak NRM made recovery of palaeomagnetic directions difficult. Stepwise AF demagnetization of the sample NRM yielded results which were too noisy for reliable determination of directions. Thermal demagnetization of other samples drilled from the same stratigraphic heights proved more successful, but still insufficient for reliable determination of the primary remanence.

Samples were demagnetized in air in a field-free oven at 25 °C intervals, until mineral alteration was detected by sudden increases in magnetic susceptibility or remanence, usually at around 300 °C. Fig. 8 comprises Zijderveld (1967) plots for four samples from within, above, and below the glauconitic horizon. The data are noisy but have clear directional trends. The trends are not directed toward the origin of the Zijderveld (1967) plots, and probably represent a viscous overprint. The component directions are very roughly aligned with the present-day field (inclination  $-70^\circ$ , declination  $25^\circ$ ; calculated GAD inclination  $-64^\circ$ ). The formation dip is around  $6^\circ$ , which – given the quality of the data – is insufficient to distinguish a present-day overprint from a normal pre-tilt remanence. While the primary magnetization is not visible, it might be recoverable using a sufficient number of samples: the great-circle remagnetization analysis technique of McFadden and McElhinny (1988) allows a primary direction to be inferred from partial demagnetization paths.

## 4. Discussion

### 4.1. Magnetic mineralogy

IRM acquisition and thermal demagnetization data indicate that magnetite carries the remanence in these sediments. It is important to establish whether this magnetite is capable of retaining a remanence over geological time-spans; for such retention, magnetite in the SD or PSD domain state is required, corresponding approximately to a grain size range of 0.03–2  $\mu\text{m}$  (Maher, 2007, p. 253). Larger grains would be in a MD state, which makes them less capable of retaining a stable remanence over millions of years.

Unblocking temperatures from stepwise demagnetization experiments indicate that the magnetite in the studied sediments is capable of retaining remanence over geological time. Néel (1955) derived an equation that describes the relationship between unblocking time and temperature for a magnetized SD grain: a remanence that unblocks over a given time at a given temperature will also unblock over a longer time at a lower temperature. Pullaiah et al. (1975) derived an explicit equation for this time–temperature equivalence for magnetite; for remanence unblocking, 4.6 Gyr at 20 °C is approximately equivalent to 20 min at 200 °C. Thus, any remanence retained by SD particles within the samples after the 200 °C heating step can be regarded as unaffected by viscous remanent magnetization (VRM). The studied samples clearly retain the majority of their initial remanence after this heating step (Fig. 5). While it is possible that not all grains in the samples are SD, this equation at least provides a rough estimate of VRM unblocking temperatures.

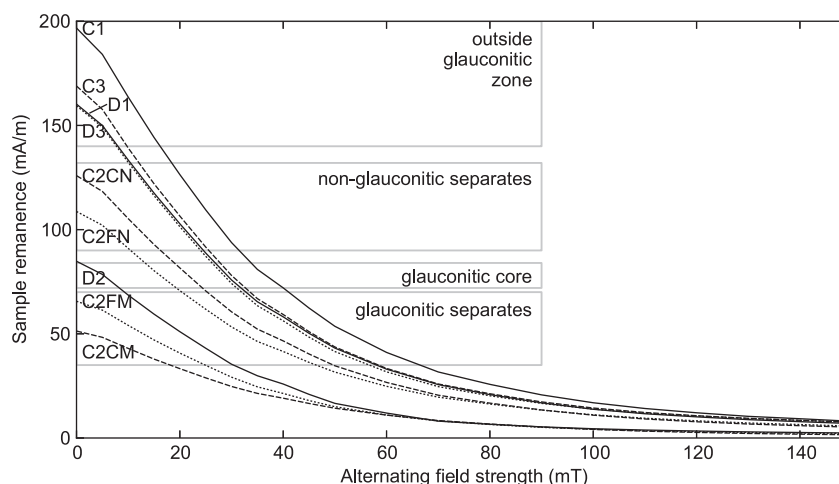
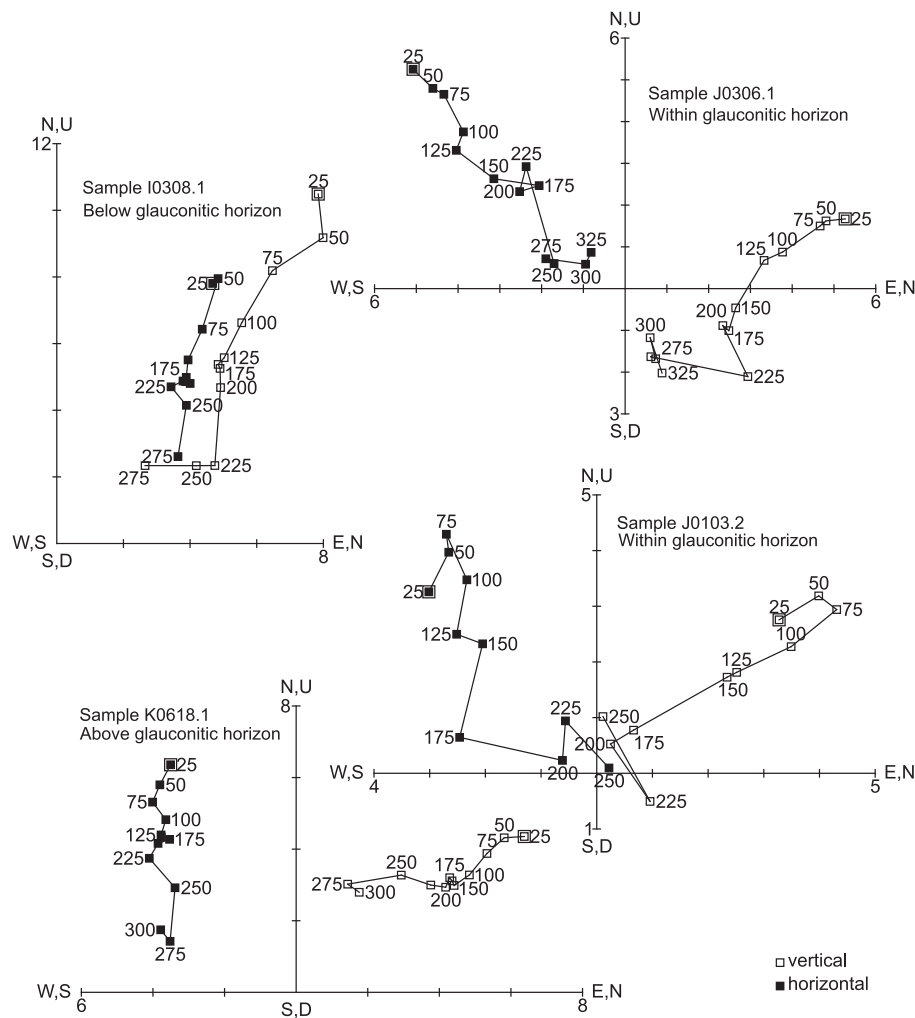


Fig. 7. Stepwise AF demagnetization of a 1 T IRM, shown for each sample group in the study.



**Fig. 8.** Zijderveld diagrams of NRM demagnetization data for samples below, within, and above the studied glauconitic horizon. The data have been corrected for bedding. Axis scales indicate magnetization in  $A/m \times 10^{-5}$ . Labels on points indicate treatment temperature in degrees Celsius. Some temperature labels are omitted for clarity. Diagrams were produced using PuffinPlot (Lurcock and Wilson, 2012).

There is also evidence for SD/PSD magnetite – and hence for stable natural remanence – from the remanent coercivities measured by DC demagnetization. In magnetite, remanent coercivity is related to grain size: the compilation of published results by Peters and Dekkers (2003) indicates that the values measured in this study (41.1–46.7 mT) correspond to a grain size range of around 0.04–2  $\mu\text{m}$ , within which SD/PSD behaviour would be expected. Further evidence of a SD/PSD domain state comes from the shape of the AF demagnetization curves, as described in Section 3.4.

Determination of the domain state of magnetite in the studied sediments provides confirmation that the samples can retain a remanence from their time of deposition. It also makes possible an estimate of the concentration of remanence carriers. For grain sizes with SD/PSD domain states, the maximum saturation remanent magnetization of magnetite is around  $4 A m^2$  (Peters and Dekkers, 2003, Fig. 2b), giving a volume-normalized magnetization of 21 kA/m. The range of SIRM values for the samples in this study is 66–199 mA/m, which corresponds to a maximum magnetite concentration of around 3–10 ppm.

Given the strong evidence for magnetite as the sole remanence carrier in the studied samples, it is somewhat surprising that they responded poorly to AF demagnetization. Marine sediments from the New Zealand region have frequently been found to respond better to thermal than to AF treatment (Kennett and Watkins, 1974; Wright and Vella, 1988; Turner et al., 1989, 2007; Roberts and Pillans, 1993). In some cases this has been attributable to a GRM acquired by greigite

(e.g. Rowan and Roberts, 2006), but in at least one case it has been associated with a well-established magnetite mineralogy (Turner et al., 2007). From the data available it is difficult to establish a cause for the poor AF response in these sediments. Dunlop and Özdemir (1997, Section 11.4.2) mentioned that spurious AF remanences have often been observed in coarse-grained rocks, and hypothesized that their weak NRM may 'highlight GRM moments carried by the fine grains'. In the studied sediments, the weak NRM may be a contributing factor, since AF treatment worked well on a strong imparted IRM (Fig. 7). It is possible that the AF behaviour is affected by a non-magnetite mineral in the samples; in this case, however, it would have to be a mineral indistinguishable from magnetite by the unblocking spectrum and remanent coercivity techniques applied in this study.

#### 4.2. Heating-induced alteration and VRM unblocking

As the thermal demagnetization of an IRM demonstrated, the magnetite grains in the studied sediments are capable of retaining a remanence up to the Curie point of 580 °C. However, stepwise demagnetization of NRM gives rise to a more complex behaviour: heating produces new minerals by 300 °C, imparting an overprint that obscures further demagnetization of the NRM. The IRM results indicate that the initial magnetite component is, as would be expected, unaffected by heating, implying that some other component of the sample is responsible for the newly-formed mineral and consequent magnetic overprint. One

candidate for this component is glauconite, which has been reported to form ferrimagnetic compounds upon heating (Mackenzie et al., 1988). Another is pyrite, which was observed to be abundant in the samples, and has previously been found to form magnetite when heated (Passier et al., 2001; Tudryn and Tucholka, 2004).

The calculations presented in Section 4.1 imply that the initial VRM should be unblocked by the 200 °C heating step, and that subsequent heating steps should therefore trend towards the origin in a direction corresponding to the primary, depositional remanence. The observed behaviour of the NRM demagnetization data, however, does not in general match this prediction. For example, no origin-directed trend is visible for sample K0618.1 (Fig. 8), even at 300 °C. We suggest two explanations for this unexpected behaviour.

- (1) The presence of PSD magnetite. The Pullaiah et al. (1975) equations are only valid for stable SD magnetite. Our rock magnetic data (MDF of IRM, AF on IRM curve shape, and remanent coercivity) are consistent with SD magnetite but do not exclude the possibility of PSD grains. PSD magnetite has previously been found to have higher VRM unblocking temperatures than those predicted by Néel theory for SD magnetite (Dunlop et al., 1997) and it is possible that, in the studied samples, the remanence remaining above 200 °C represents a VRM component carried by PSD grains.
- (2) Thermally-induced mineral alteration below 300 °C. We used bulk magnetic susceptibility to detect the formation of new ferrimagnetic minerals during heating, as is common in thermal demagnetization studies. However, this technique is rendered less effective by the high paramagnetic susceptibility of the samples and the low concentration of the original ferrimagnetic remanence carriers. This means that only a small proportion of the total susceptibility is due to magnetite. If, say, the total magnetite content of the samples were doubled by heating-induced alteration of clay minerals, the susceptibility due to magnetite would also be doubled; however, the proportional increase in the total susceptibility of the samples would be relatively small. It is therefore possible that a new magnetic mineral formed by 200 °C, producing an overprint on the remaining NRM.

In some previous studies of New Zealand sediments (Wilson and Roberts, 1999; Turner, 2001; Rowan and Roberts, 2006), high-temperature overprints have been attributed to the presence of haematite produced by oxidation of pyrite (by oxic groundwater, for instance). In the studied sediments, this explanation seems unlikely, because the measured remanent coercivities and unblocking temperatures were too low to be consistent with haematite.

#### 4.3. Relationship between glaucony and magnetization

An inverse correlation between glauconitic content and saturation magnetization is observed for D-series (drill core) samples. This suggests that glauconitic grains do not carry any magnetization, although it would still be possible to attribute these differences to some other stratigraphic mineralogical variation. Comparisons between glauconitic and non-glauconitic separates, however, give a stronger indication that it is the glauconite that dilutes the remanence.

It is the high-susceptibility ('magnetic') fraction that carries the least remanence. Most magnetic separation studies have the opposite outcome; high-field magnetic separation is often used with the implicit assumption that remanence carriers will be concentrated in the high-susceptibility fraction (Hounslow and Maher, 1996). The opposite outcome in this study is due in part to the high concentration of glauconite, which has a high paramagnetic susceptibility. However, this alone cannot account for the separation results because pure magnetite has a much higher susceptibility than glauconitic grains. The concentration of magnetite in the low-susceptibility fraction implies that the

magnetite grains must be physically attached to or embedded in larger, low-susceptibility grains, which effectively dilute their susceptibility.

The observed high glauconite content and low magnetite concentration can complicate rock magnetic calculations. For example, when using the 'King plot' (King et al., 1982), it is assumed that the susceptibility of a sample is dominated by magnetite. For many natural samples, this is the case, but the assumption is often made in cases where it does not hold (Yamazaki and Ioka, 1997). For highly glauconitic samples with high paramagnetic susceptibility and low concentrations of remanence carriers, it is an invalid assumption.

#### 4.4. Remanence acquisition model

The magnetite-dominated magnetic mineralogy and reducing depositional environment (which is indicated by the widespread presence of pyrite in the studied samples) imply a fairly straightforward model of remanence acquisition: detrital magnetite grains acquired a depositional remanent magnetization, which was then substantially weakened by dissolution of most of the magnetite. However, the model needs to account for survival of a small proportion of the detrital magnetite. This survival could be explained by one of two processes:

- (1) Pyritization may have been arrested by a lack of hydrogen sulphide to react with iron.
- (2) The magnetite may have been physically protected in some way from contact with corrosive sulphidic pore waters.

##### 4.4.1. Process 1: excess magnetite

Process 1 is generally consistent with the conclusions of Berner (1970) and Kao et al. (2004), who found that iron is most often (though not always) in excess during pyritization reactions, so that the extent of pyritization is controlled by the availability of organic matter and sulphate. A form of process 1 was adopted by Roberts and Turner (1993) to account for preservation of a low concentration of titanomagnetite grains in Neogene sediments from New Zealand: they suggested that a high sedimentation rate limited downward diffusion of sulphate from sea-water, and that the original amount of detrital iron was more than sufficient to react with all the available sulphate under these conditions.

For our samples, however, this hypothesis seems unlikely, for several reasons. One problem is the lack of intermediate sulphides such as greigite that would be expected if pyritization had been arrested (Roberts and Turner, 1993). Another problem is the low concentration of magnetite: this would imply that – at least in the studied interval – the amount of available sulphide was precisely sufficient to dissolve all but a few parts per million of the available magnetite. Such a close correspondence between the quantities of the reactants is implausible.

This hypothesis also fails to account for the inferred grain size of the magnetite: in general, smaller magnetite grains should be dissolved first due to their higher surface area to volume ratio. Thus, once pyritization is well advanced, the remaining detrital magnetite grains should be the largest ones; this situation has been observed by, for example, Karlin (1990) and Rowan and Roberts (2006). Such observations are difficult to reconcile with the inferred SD/PSD (<2 µm) grain size of the magnetite in these samples.

##### 4.4.2. Process 2: protected magnetite

Process 2 is consistent with the fact that the remanence appears to be carried by the grains with lower susceptibility; this could be explained by the presence of magnetite inclusions within weakly paramagnetic or diamagnetic grains. Magnetite inclusions have long been known to occur within silicate minerals in igneous rocks (e.g. Evans et al., 1968; Davis, 1981; Bogue et al., 1995; Feinberg et al., 2005); more recently, their counterparts in sedimentary silicates have also been investigated (e.g. Hounslow et al., 1995). Hounslow and Morton (2004) defined four classes of iron oxide inclusions

within sedimentary particles. For palaeomagnetic purposes, the most important distinction is between two main types of inclusion: first, inclusions that formed in a source rock before being transported and deposited as sediment; and second, inclusions that formed in situ as a result of authigenic mineral growth. This distinction is important for detrital remanent magnetization (DRM) acquisition. The orientation of a magnetized grain settling onto an underwater surface is controlled by several factors: the torque exerted by the ambient magnetic field; the inertia of the grain; viscous torque from the water; and the torque resulting from contact with the surface (Dunlop and Özdemir, 1997, Section 15.2). Theoretical and experimental results indicate that, for pure SD and PSD magnetite grains, the magnetic force dominates, which allows the grain to align with the geomagnetic field and preserve a DRM. However, if magnetite is present only as inclusions within a larger grain, the magnetic torque will be correspondingly weaker and is unlikely to be sufficient to overcome mechanical, inertial, and viscous forces. If, conversely, the inclusion is formed post-depositionally, the process of DRM acquisition should be unaffected. Heslop (2007) described a model for the settling of flocs containing magnetized particles; his results suggested that magnetic torque would have a negligible effect on flocs larger than 12  $\mu\text{m}$ .

Both types of inclusion have been reported. Canfield and Berner (1987) found that in some cases pyrite overgrows magnetite grains, which protects the magnetite from further sulphidization. Karlin (1990) reported growth of protective coatings of amorphous silica on magnetite, and Rowan and Roberts (2006) found similar pyrite coatings protecting greigite from further pyritization and allowing it to retain a remanence from its time of formation. Hounslow et al. (1995) described magnetic inclusions in sedimentary quartz. In this case, the quartz protected the inclusions (inferred to be magnetite) from pyritization, but it appeared unlikely that they could carry a reliable palaeomagnetic remanence, due to the dominance of hydrodynamic forces on the settling grains. Maher and Hallam (2005) found abundant magnetic inclusions within silicates in Pleistocene North Sea sediments, and concluded that they carried a negligible palaeomagnetic signal.

Wilson and Roberts (1999) studied heavily pyritized sediments whose remanence was apparently carried by ilmenite grains, despite the fact that ilmenite is paramagnetic. They concluded that the ilmenite contained sub-micron ferrimagnetic iron-enriched zones with a probable haemo-ilmenite mineralogy. The unreactive ilmenite was inferred to have protected the ferrimagnetic zones from the strongly reducing conditions, and – given the preservation of a palaeomagnetic signal – the overall magnetic moment had evidently been sufficient to align the entire grain. While this is unlikely to be an efficient magnetization, it is likely that the finest such particles are responsible for the palaeomagnetic signal.

In the samples analysed in this study, magnetite concentrations are low, so the ‘protected magnetite’ hypothesis does not require inclusions to be common; only a small proportion of the original detrital magnetite needs to survive to carry the observed weak NRMs. In our samples, as with many of the studies described above, magnetic inclusions were not directly observed, but were inferred from rock magnetic and sedimentological data. It is, thus, impossible to say from direct analysis whether the inferred inclusions formed in situ, which allows them to record a palaeomagnetic direction, or whether magnetite grains were deposited within pre-existing inclusions, which would mean that the orientation was controlled mainly by mechanical rather than magnetic forces. However, studies such as that by Karlin (1990) show that inclusions have the potential to preserve magnetization in sediments. In a palaeomagnetic study, the reliability of the remanence can be confirmed by subjecting measured palaeomagnetic directions to standard palaeomagnetic tests, such as consistency between samples, alignment with a known palaeofield direction, the reversals test (Cox and Doell, 1960), or the fold test of Graham (1949).

Since our separation of glauconitic material was not complete, there remains the possibility that some remanence was carried by magnetite

grains incorporated within glauconitic particles. Even in this case, however, an approximately syndepositional remanence would be expected, since the magnetite would have to be locked in early enough to escape pyritization.

#### 4.5. Origin of the magnetite

The two CLG coercivity components observed in the IRM acquisition data have some similarity to the BS and BH (biogenic soft and biogenic hard) components identified in the coercivity studies of Egli (2004). In recent years, biogenic magnetite has been increasingly reported in ancient sediments (e.g. Yamazaki, 2008; Yamazaki, 2009; Roberts et al., 2011a; Roberts et al., 2012; Larrasoana et al., 2012). A biogenic origin would indicate that the magnetite formed in situ. The grain size and shape of biogenic magnetite are ideal for recording palaeomagnetic signals. Also, the small grain size implies that biogenic magnetite would dissolve swiftly in a reducing environment, which implies that any surviving biogenic magnetite must have been protected, and its remanence locked in, soon after formation. Identification of a biogenic origin for the magnetite would, thus, provide strong corroboration for its fidelity as a remanence carrier.

The coercivity data presented in this paper, while suggestive of biogenic magnetite, cannot be firmly identified with the BS and BH components of Egli (2004), which are defined in terms of skewed generalized Gaussian (SGG) distribution functions rather than (as in this paper) unskewed Gaussian functions. Reliable identification of the BS and BH components also requires use of anhysteretic remanent magnetization (ARM) data. Analysis using the techniques of Egli (2004) and Egli et al. (2010) would be a useful future extension of this study.

## 5. Conclusions

Glauconitic sediments have the potential to record a stable palaeomagnetic remanence, which is locked in at the time of deposition rather than during the glauconitization process. By comparing the rock magnetic properties of glauconitic and non-glauconitic strata, and of glauconitic and non-glauconitic separates from the same stratum, we have established that the glauconitic grains do not hold a magnetic remanence. In the studied sediments, remanence is carried by a low concentration of single-domain or pseudo-single-domain magnetite that was apparently protected from pyritization by encapsulation within an inert, paramagnetic or diamagnetic mineral.

Although the primary magnetization is inferred to be stable, measuring it accurately presents significant challenges. As with many New Zealand sediments, AF demagnetization produces spurious remanences, which here are difficult to explain in terms of the magnetite mineralogy. Thermal demagnetization produces better results, but can only be continued to around 300 °C before the NRM is obscured by new magnetic minerals produced by heating-induced alteration. This problem is compounded by the high paramagnetic susceptibility of the glauconitic component, which reduces the sensitivity of the standard susceptibility measurement technique for monitoring alteration. In the studied sediments, these factors prevented the reliable determination of the original remanence direction. Our results imply that the presence of glauconite causes problems in the measurement of a primary remanence rather than in its preservation, especially when the concentration of remanence carriers is very low. While these results cannot automatically be generalized to all glauconitic sediments, they indicate that heavily glauconitized sediments can be difficult, but not necessarily impossible, targets for palaeomagnetic investigation. Glauconitic intervals are commonly associated with variations in bottom-water flow and terrigenous input, so dating them palaeomagnetically can provide accurate age constraints on the geological events that they record.

## Acknowledgements

We thank Christian Ohneiser, Claudio Tapia, and Bob Dagg for field assistance; Brent Pooley for producing the thin sections for micro-analysis; Andreas Auer for assistance with the electron microprobe; and Christian Ohneiser for valuable comments on an early draft of this paper. We also thank Andrew Roberts and an anonymous reviewer for many improvements to the manuscript. This work was funded by University of Otago research grants to GSW and a University of Otago scholarship held by PCL.

## References

- Amorosi, A., 1995. Glaucony and sequence stratigraphy: a conceptual framework of distribution in siliciclastic sequences. *Journal of Sedimentary Research* 65, 419–425.
- Amorosi, A., Sammartino, I., Tateo, F., 2007. Evolution patterns of glaucony maturity: a mineralogical and geochemical approach. *Deep Sea Research II* 54, 1364–1374.
- Bentor, Y.K., Kastner, M., 1965. Notes on the mineralogy and origin of glauconite. *Journal of Sedimentary Research* 35, 155–166.
- Berner, R.A., 1970. Sedimentary pyrite formation. *American Journal of Science* 268, 1–23.
- Bogue, S.W., Grommé, S., Hillhouse, J.W., 1995. Paleomagnetism, magnetic anisotropy, and mid-Cretaceous paleolatitude of the Duke Island (Alaska) ultramafic complex. *Tectonics* 14, 1133–1152.
- Canfield, D.E., Berner, R.A., 1987. Dissolution and pyritization of magnetite in anoxic marine sediments. *Geochimica et Cosmochimica Acta* 51, 645–659.
- Cox, A., Doell, R.R., 1960. Review of paleomagnetism. *Geological Society of America Bulletin* 71, 645–768.
- Davis, K.E., 1981. Magnetite rods in plagioclase as the primary carrier of stable NRM in ocean floor gabbros. *Earth and Planetary Science Letters* 55, 190–198.
- Dekkers, M.J., 1989. Magnetic properties of natural pyrrhotite II. High- and low-temperature behaviour of  $J_s$  and TRM as function of grain size. *Physics of the Earth and Planetary Interiors* 57, 266–283.
- Dunlop, D.J., 1986. Coercive forces and coercivity spectra of submicron magnetites. *Earth and Planetary Science Letters* 78, 288–295.
- Dunlop, D.J., Özdemir, Ö., 1997. *Rock Magnetism: Fundamentals and Frontiers*. Cambridge Studies in Magnetism, 3. Cambridge University Press.
- Dunlop, D.J., Özdemir, Ö., Schmidt, P.W., 1997. Paleomagnetism and paleothermometry of the Sydney Basin 2. Origin of anomalously high unblocking temperatures. *Journal of Geophysical Research: Solid Earth* 102, 27285–27295.
- Egli, R., 2003. Analysis of the field dependence of remanent magnetization curves. *Journal of Geophysical Research* 108, 2081. <http://dx.doi.org/10.1029/2002JB002023>.
- Egli, R., 2004. Characterization of individual rock magnetic components by analysis of remanence curves, 1. unmixing natural sediments. *Studia Geophysica et Geodaetica* 48, 391–446.
- Egli, R., Chen, A., Winklhofer, M., Kodama, K.P., Hornig, C.S., 2010. Detection of non-interacting single domain particles using first-order reversal curve (FORC) diagrams. *Geochemistry, Geophysics, Geosystems* 11, Q01Z11. <http://dx.doi.org/10.1029/2009GC002916>.
- Evans, M.E., McElhinny, M.W., Gifford, A.C., 1968. Single domain magnetite and high coercivities in a gabbroic intrusion. *Earth and Planetary Science Letters* 4, 142–146.
- Feinberg, J.M., Scott, G.R., Renne, P.R., Wenk, H.R., 2005. Exsolved magnetite inclusions in silicates: features determining their remanence behavior. *Geology* 33, 513–516.
- Goldman, M.I., 1922. Basal glauconite and phosphate beds. *Science* 56, 171–173.
- Graham, J.W., 1949. The stability and significance of magnetism in sedimentary rocks. *Journal of Geophysical Research* 54, 131–167.
- Heslop, D., 2007. Are hydrodynamic shape effects important when modelling the formation of depositional remanent magnetization? *Geophysical Journal International* 171, 1029–1035.
- Heslop, D., Dekkers, M.J., Kruiver, P.P., Van Oorschot, I.H.M., 2002. Analysis of isothermal remanent magnetization acquisition curves using the expectation–maximization algorithm. *Geophysical Journal International* 148, 58–64.
- Hesselbo, S.P., Huggett, J.M., 2001. Glaucony in ocean-margin sequence stratigraphy (Oligocene–Pliocene, offshore New Jersey, USA; ODP leg 174A). *Journal of Sedimentary Research* 71, 599–607.
- Hopkinson, J., 1889. Magnetic and other physical properties of iron at a high temperature. *Philosophical Transactions of the Royal Society of London. A* 180, 443–465.
- Hounslow, M.W., Maher, B.A., 1996. Quantitative extraction and analysis of carriers of magnetization in sediments. *Geophysical Journal International* 124, 57–74.
- Hounslow, M.W., Morton, A.C., 2004. Evaluation of sediment provenance using magnetic mineral inclusions in clastic silicates: comparison with heavy mineral analysis. *Sedimentary Geology* 171, 13–36.
- Hounslow, M.W., Maher, B.A., Thistlewood, L., 1995. Magnetic mineralogy of sandstones from the Lunde Formation (late Triassic), northern North Sea, UK: origin of the palaeomagnetic signal. In: Turner, P., Turner, A. (Eds.), *Palaeomagnetic Applications in Hydrocarbon Exploration and Production*. Geological Society Special Publications, 98, pp. 119–147.
- Hrouda, F., 2003. Indices for numerical characterization of the alteration processes of magnetic minerals taking place during investigation of temperature variation of magnetic susceptibility. *Studia Geophysica et Geodaetica* 47, 847–861.
- Huggett, J.M., 2005. Glauconites. In: Selley, R.C., Cocks, L.R.M., Plimer, I.R. (Eds.), *Encyclopedia of Geology*. Elsevier, pp. 542–548.
- Hunt, C.P., Moskowitz, B.M., Banerjee, S.K., 1995. Magnetic properties of rocks and minerals. In: Ahrens, T.J. (Ed.), *Rock physics and phase relations: a handbook of physical constants*. American Geophysical Union, pp. 189–204.
- Kao, S.J., Hornig, C.S., Roberts, A.P., Liu, K.K., 2004. Carbon–sulfur–iron relationships in sedimentary rocks from southwestern Taiwan: influence of geochemical environment on greigite and pyrrhotite formation. *Chemical Geology* 203, 153–168.
- Karlin, R., 1990. Magnetite diagenesis in marine sediments from the Oregon continental margin. *Journal of Geophysical Research* 95, 4405–4419.
- Kennett, J.P., Watkins, N.D., 1974. Late Miocene–early Pliocene paleomagnetic stratigraphy, paleoclimatology, and biostratigraphy in New Zealand. *Geological Society of America Bulletin* 85, 1385–1398.
- King, J., Banerjee, S.K., Marvin, J., Özdemir, Ö., 1982. A comparison of different magnetic methods for determining the relative grain size of magnetite in natural materials: some results from lake sediments. *Earth and Planetary Science Letters* 59, 404–419.
- Kostadinova, M., Jordanova, N., Jordanova, D., Kovacheva, M., 2004. Preliminary study on the effect of water glass impregnation on the rock-magnetic properties of baked clay. *Studia Geophysica et Geodaetica* 48, 637–646.
- Kruiver, P.P., Dekkers, M.J., Heslop, D., 2001. Quantification of magnetic coercivity components by the analysis of acquisition curves of isothermal remanent magnetisation. *Earth and Planetary Science Letters* 189, 269–276.
- Larrasoña, J.C., Roberts, A.P., Chang, L., Schellenberg, S.A., Fitz Gerald, J.D., Norris, R.D., Zachos, J.C., 2012. Magnetotactic bacterial response to Antarctic dust supply during the Palaeocene–Eocene thermal maximum. *Earth and Planetary Science Letters* 333–334, 122–133.
- Li, H.Y., Zhang, S.H., 2005. Detection of mineralogical changes in pyrite using measurements of temperature-dependence susceptibilities. *Chinese Journal of Geophysics* 48, 1454–1461.
- Lowrie, W., 1990. Identification of ferromagnetic minerals in a rock by coercivity and unblocking temperature properties. *Geophysical Research Letters* 17, 159–162.
- Lurcock, P.C., Wilson, G.S., 2012. Puffinplot: a versatile, user-friendly program for paleomagnetic analysis. *Geochemistry, Geophysics, Geosystems* 13, Q06Z45. <http://dx.doi.org/10.1029/2012GC004098>.
- Mackenzie, K.J.D., Cardile, C.M., Brown, I.W.M., 1988. Thermal and Mössbauer studies of iron-containing hydrous silicates: VII. glauconite. *Thermochimica Acta* 136, 247–261.
- Maher, B.A., 2007. Environmental magnetism and climate change. *Contemporary Physics* 48, 247–274.
- Maher, B.A., Hallam, D.F., 2005. Magnetic carriers and remanence mechanisms in magnetite–poor sediments of Pleistocene age, southern North Sea margin. *Journal of Quaternary Science* 20, 79–94.
- McFadden, P.L., McElhinny, M.W., 1988. The combined analysis of remagnetization circles and direct observations in palaeomagnetism. *Earth and Planetary Science Letters* 87, 161–172.
- McMillan, S.G., Wilson, G.J., 1997. Allostratigraphy of coastal south and east Otago: a stratigraphic framework for interpretation of the Great South Basin, New Zealand. *New Zealand Journal of Geology and Geophysics* 40, 91–107.
- Mitchum Jr., R.M., Van Wagoner, J.C., 1991. High-frequency sequences and their stacking patterns: sequence-stratigraphic evidence of high-frequency eustatic cycles. *Sedimentary Geology* 70, 131–160.
- Néel, L., 1955. Some theoretical aspects of rock-magnetism. *Advances in Physics* 4, 191–243.
- Odin, G.S., 1982. How to measure glaucony ages. In: Odin, G.S. (Ed.), *Numerical Dating in Stratigraphy, Part 1*. Wiley, New York, pp. 387–403 (volume 1, chapter 20).
- Odin, G.S., Matter, A., 1981. De glauconiarum origine. *Sedimentology* 28, 611–641.
- Passier, H.F., De Lange, G.J., Dekkers, M.J., 2001. Magnetic properties and geochemistry of the active oxidation front and the youngest sapropel in the eastern Mediterranean Sea. *Geophysical Journal International* 145, 604–614.
- Peters, C., Dekkers, M.J., 2003. Selected room temperature magnetic parameters as a function of mineralogy, concentration and grain size. *Physics and Chemistry of the Earth, Parts A/B/C* 28, 659–667.
- Pullaiah, G., Irving, E., Buchan, K.L., Dunlop, D.J., 1975. Magnetization changes caused by burial and uplift. *Earth and Planetary Science Letters* 28, 133–143.
- Roberts, A.P., Pillans, B.J., 1993. Rock magnetism of Lower/Middle Pleistocene marine sediments, Wanganui Basin, New Zealand. *Geophysical Research Letters* 20, 839–842.
- Roberts, A.P., Turner, G.M., 1993. Diagenetic formation of ferrimagnetic iron sulphide minerals in rapidly deposited marine sediments, South Island, New Zealand. *Earth and Planetary Science Letters* 115, 257–273.
- Roberts, A.P., Florindo, F., Villa, G., Chang, L., Jovane, L., Bohaty, S.M., Larrasoña, J.C., Heslop, D., Fitz Gerald, J.D., 2011a. Magnetotactic bacterial abundance in pelagic marine environments is limited by organic carbon flux and availability of dissolved iron. *Earth and Planetary Science Letters* 310, 441–452.
- Roberts, A.P., Chang, L., Rowan, C.J., Hornig, C.S., Florindo, F., Reviews of Geophysics, 2011b. Magnetic properties of sedimentary greigite (Fe<sub>3</sub>O<sub>4</sub>): an update. *Reviews of Geophysics* 49, RG1002. <http://dx.doi.org/10.1029/2010RG000336>.
- Roberts, A.P., Chang, L., Heslop, D., Florindo, F., Larrasoña, J.C., 2012. Searching for single domain magnetite in the “pseudo-single-domain” sedimentary haystack: implications of biogenic magnetite preservation for sediment magnetism and relative paleointensity determinations. *Journal of Geophysical Research: Solid Earth* 117. <http://dx.doi.org/10.1029/2012JB009412> B08104.
- Robertson, D.J., France, D.E., 1994. Discrimination of remanence-carrying minerals in mixtures, using isothermal remanent magnetisation acquisition curves. *Physics of the Earth and Planetary Interiors* 82, 223–234.
- Rowan, C.J., Roberts, A.P., 2006. Magnetite dissolution, diachronous greigite formation, and secondary magnetizations from pyrite oxidation: unravelling complex magnetizations in Neogene marine sediments from New Zealand. *Earth and Planetary Science Letters* 241, 119–137.
- Symons, D.T.A., Cioppa, M.T., 2000. Crossover plots: a useful method for plotting SIRM data in paleomagnetism. *Geophysical Research Letters* 27, 1779–1782.
- Tudryn, A., Tucholka, P., 2004. Magnetic monitoring of thermal alteration for natural pyrite and greigite. *Acta Geophysica Polonica* 52, 509–520.

- Turner, G.M., 2001. Toward an understanding of the multicomponent magnetization of uplifted Neogene marine sediments in New Zealand. *Journal of Geophysical Research* 106, 6385–6397.
- Turner, G.M., Roberts, A.P., Laj, C., Kissel, C., Mazaud, A., Guitton, S., Cristoffel, D.A., 1989. New paleomagnetic results from Blind River: revised magnetostratigraphy and tectonic rotation of the Marlborough region, South Island, New Zealand. *New Zealand Journal of Geology and Geophysics* 32, 191–196.
- Turner, G.M., Michalk, D.M., Morgans, H.E.G., Walbrecker, J.O., 2007. Early Miocene magnetostratigraphy and a new palaeomagnetic pole position from New Zealand. *Earth, Planets and Space* 59, 841–851.
- Wang, L., Pan, Y., Li, J., Qin, H., 2008. Magnetic properties related to thermal treatment of pyrite. *Science in China Series D: Earth Sciences* 51, 1144–1153.
- Wilson, G.S., Roberts, A.P., 1999. Diagenesis of magnetic mineral assemblages in multiply redeposited siliciclastic marine sediments, Wanganui basin, New Zealand. In: Tarling, D.H., Turner, P. (Eds.), *Palaeomagnetism and Diagenesis in Sediments*. Geological Society Special Publications, 151, pp. 95–108.
- Wright, I.C., Vella, P.P., 1988. A New Zealand Late Miocene magnetostratigraphy: glacioeustatic and biostratigraphic correlations. *Earth and Planetary Science Letters* 87, 193–204.
- Yamazaki, T., 2008. Magnetostatic interactions in deep-sea sediments inferred from first-order reversal curve diagrams: implications for relative paleointensity normalization. *Geochemistry, Geophysics, Geosystems* 9. <http://dx.doi.org/10.1029/2007GC001797>. Q02005.
- Yamazaki, T., 2009. Environmental magnetism of Pleistocene sediments in the North Pacific and Ontong–Java Plateau: temporal variations of detrital and biogenic components. *Geochemistry, Geophysics, Geosystems* 10, Q07Z04. <http://dx.doi.org/10.1029/2009GC002413>.
- Yamazaki, T., Ioka, N., 1997. Cautionary note on magnetic grain-size estimation using the ratio of ARM to magnetic susceptibility. *Geophysical Research Letters* 24, 751–754.
- Zijderveld, J.D.A., 1967. A.C. demagnetization of rocks: analysis of results. In: Collinson, D.W., Creer, K.M., Runcorn, S.K. (Eds.), *Methods in Palaeomagnetism*. Elsevier, pp. 254–286.